Nanoscale

Accepted Manuscript

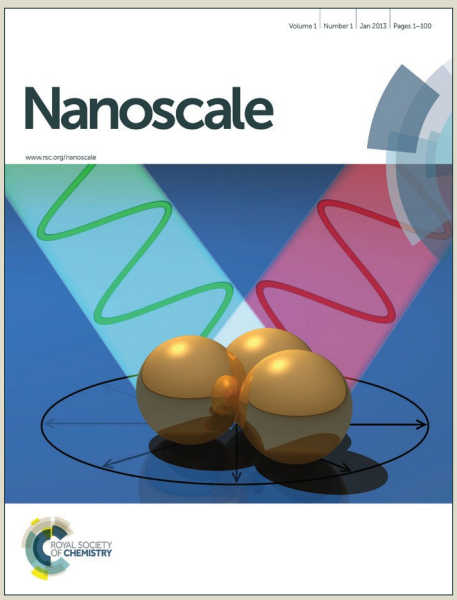

ROYAL SOCIETY OF CHEMISTRY

www.rsc.org/nanoscale

Journal Name

ARTICLE

Superior Oxygen Reduction Electrocatalysis Enabled by Integrating Hierarchical Pores, Fe_3C Nanoparticles and Bamboo-like Carbon Nanotubes

Received 00th January 20xx,
Accepted 00th January 20xx

DOI: 10.1039/x0xx00000x
www.rsc.org/

Wenxiu Yang, [a,c] Xiaoyu Yue, [a,c] Xiangjian Liu, [a,c] Lulu Chen, [a,c] Jianbo Jia *,[a] and Shaojun Guo *,[b]

Hierarchical porous carbon nanostructures doped with nitrogen or other active elements have been demonstrated to be an important direction in enhancing the oxygen reduction reaction (ORR) activity. However, their intrinsic limited active sites usually make them have lower ORR activity than that of commercial Pt/C. In order to well solve this challenging issue, herein we develop a simple method for encapsulating more electrochemically active Fe_3C nanoparticles (NPs) into the channels of bamboo-like carbon nanotubes (bCNTs) with interesting 3D hierarchical micro-, meso- and macropores by impregnating the bCNTs with $Fe(NO_3)_3$ solution, and followed by the calcination of composite in N_2 atmosphere. The resulting bCNT/Fe_3C hybrid electrocatalysts with much more active sites exhibit excellent ORR activity in acidic media with the half-wave potential of 0.710 V comparable to that of the commercial Pt/C catalyst (0.782 V). Furthermore, they show very high ORR activity in 0.10 M KOH with the half-wave potential of 0.879 V, 67 mV more positive than that of Pt/C catalyst. Most importantly, the as-prepared new catalysts are very stable for ORR in both acidic and alkaline solutions with almost no ORR polarization curve shift after 3000 cycles, much better than that of the Pt/C catalyst. To the best of our knowledge, our new bCNT/Fe_3C catalyst is the best non-noble-metal catalysts ever reported for ORR in both acidic and alkaline conditions. The present work highlights the important roles of introducing more stable Fe_3C NPs and hierarchical micro-, meso- and macropores as much more active sites for maximizing ORR electrocatalysis performance.

Introduction

The development of low-cost, active and durable oxygen reduction reaction (ORR) nanocatalysts is indispensable for the future sustainable energy devices such as fuel cells and metal-air batteries.[1-4] Doping carbon nanomaterials with N or other active elements (*e.g.* B, S, and P) has been suggested to be an effective way for enhancing ORR activity.[5-11] Unfortunately, even though great efforts have been devoted to designing more rational three-dimensional (3D) porous carbon nanomaterials with the proper nitrogen doping or even multiple active elements doping, their ORR activities are still limited, and usually inferior to that of commercial Pt/C catalyst.[12-16] To explore more active non-noble metal catalysts, recent advances have moved onto the design of carbon nanomaterials/transition metal oxide nanoparticles (NPs) composites for further enhancing ORR activity.[6, 17, 18] Under the optimal conditions, a few of composite catalysts can have the similar or identical ORR activity as that of Pt/C catalyst, but still be not more active for ORR than Pt/C.[19, 20] This challenging issue has been initially resolved by developing a large-scale protocol for the controlled synthesis of the most efficient bamboo-like carbon nanotube (bCNT)/Fe_3C NPs (named as PMF because the raw materials are a mixture of PEG-PPG-PEG Pluronic® P123, melamine, and $Fe(NO_3)_3$) hybrid nanoelectrocatalysts, showing a 49 mV more positive half-wave potential for ORR than that of Pt/C catalyst in alkaline solution.[21] Despite the great potential in significantly enhancing ORR activity, the PMF still suffers from the limited transfer pathway and low Fe_3C loading amount, greatly restricting its ORR activity especially in acidic

[a] State Key Laboratory of Electroanalytical Chemistry, Changchun Institute of Applied Chemistry, Chinese Academy of Sciences, Changchun, Jilin 130022, China E-mail : jbjia@ciac.ac.cn
[b] Department of Materials Science & Engineering, & Department of Energy and Resources Engineering, College of Engineering, Peking University, Beijing 100871, China. E-mail: sjguo@coe.pku.edu.cn; guosj@pku.edu.cn
[c] University of Chinese Academy of Sciences, Beijing 100049, China
Electronic supplementary information (ESI) available: Supplementary figures and tables. See DOI:

solution (**Scheme 1**). In this regards, exploring more effective methods to introduce 3D diffusion pathway for O_2 and electrolyte with more electrochemical active and stable Fe_3C NPs into bCNTs may be the key to get extremely active and stable non-noble metal catalysts for ORR in both acidic and alkaline solutions, but is still a great challenge.

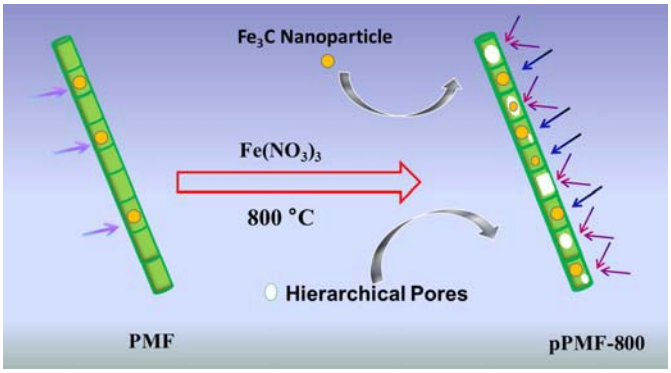

Scheme 1. Schematic illustration on introducing hierarchical pores and more electrochemically active Fe_3C NPs onto/into the bCNTs.

By taking the advantage of PMF in enhancing ORR performance, herein, we design a very simple method for manufacturing hierarchical micro-, meso-, and macropores on the walls of bCNTs additionally with more electrochemically active Fe_3C nanoparticles (NPs) (very different from PMF with only microspores) by first impregnating the PMF with $Fe(NO_3)_3$ solution and then calcination in N_2 atmosphere at 800 ^oC. The as-prepared porous PMF (renamed as pPMF-X (X is the pyrolysis temperature)) shows sufficient hierarchical pores and also more active Fe_3C NPs onto/into the bCNTs for enhancing ORR performance in both acidic and alkaline solutions **(Scheme 1)**. These two additional important features make the pPMF-800 exhibit a very high ORR activity and superior durability relative to the previous best PMF catalyst and commercial Pt/C catalyst in both acidic and alkaline solutions. It has an excellent ORR half-wave potential ($E_{1/2}$) (0.710 V) (*vs.* reversible hydrogen electrode (RHE)), which is comparable to that of the Pt/C catalyst 0.782 V in acidic solution. In particular, the $E_{1/2}$ of pPMF-800 for ORR is 0.879 V in 0.10 M KOH, which is 67 mV more positive than that of 20 wt% Pt/C ($E_{1/2}$ of 0.812 V). Furthermore, the resulting pPMF-800 exhibits much higher stability, with almost no ORR polarization curve shift in both acidic and alkaline solutions, much better than those of the Pt/C catalyst. The new pPMF-800 presented here is the most efficient non-noble-metal catalysts ever reported for ORR.

.

Experimental Section

Materials. PEG-PPG-PEG Pluronic® P123 (Mw = 5800) a Nafion (5.0 wt %) were purchased from Sigma-Aldrich. Iro nitrate, perchloric acid, and potassium hydroxide wer obtained from Beijing Chemical Reagent Company (Beij China). Melamine was purchased from the Guangfu Chemic Reagent Company. Pt catalyst (20 wt %, Pt/C) was purchase from Johnson Matthey. NCNT was brought from the Nanjing XFNANO Materials Tech Co., Ltd (XFNANO, China). A aqueous solutions were prepared with ultrapure water from a Water Purifier System (Sichuan Water Purifier Co. Ltd., China).

Apparatus. TEM measurements were made on HITACHI H-8100 and JEM-2100F high-resolution transmission electro microscope (JEOL Ltd., Japan). XRD was obtained with model D8 ADVANCE (BRUKER, Cu K_α radiation, λ =1.5406 Å). TGA was measured with NETZSCH STA 449 Nitrogen sorption isotherms were performed with an ASAP 2020 Physisorption Analyzer (Micrometrics Instrumer Corporation). Raman spectra were measured with a Renishaw 2000 model confocal microscopy Raman spectrometer with CCD detector and a holographic notch filter (Renishaw Ltd Gloucestershire, U. K.). XPS analysis was performed on a ESCALABMKII X-ray photoelectron spectrometer (V Scientific, UK). The electrochemical experiments were performed using a CHI842B electrochemical workstation (C Instruments, Shanghai). Rotating ring-disk electrode (RRDE techniques were employed on a Model RRDE-3A Apparatus (ALS, Japan) with a CHI842B electrochemical workstatio The electrochemical experiments were carried out *via* a three electrode system with a modified glassy carbon electrod as the working electrode, an Ag/AgCl (saturated KCl) electrode as the reference electrode, and a platinum foil as the counter electrode, respectively. Meanwhile, the potential whic measured against the Ag/AgCl electrode, was converted to the potential versus the reversible hydrogen electrode (RHE) according to E(*vs* RHE) = E(*vs* Ag/AgCl) + 0.197 + 0.059pH. All the potentials reported in our work were *vs* RHE. All th measurements were performed out at room temperature.

Synthesis of pPMF-800. The BCNFNHs were synthesized according to our previous reported procedure.[21] Then, the were mixed with 1.0 wt% $Fe(NO_3)_3$ solution for 12 h, and dried at 60 °C for 12 h. The pPMF-800 was obtained b heating the above powder at 180, 240, and 800 °C for 2, 2 and 1 h at a heating rate of 2 °C/min, respectively in a quar boat in N_2. For a comparison, NCNT-800-Fe was prepared b the same method with NCNT and 1.0 wt% $Fe(NO_3)_3$ solutio

To clarify, the resulting sample was labeled as pPMF-X considering the porous microstructure, PMF precursor and the pyrolysis temperature (600, 700, and 800 °C).

To further study the effect of concentration of $Fe(NO_3)_3$ solution on the resulting composites, a series of materials were produced through the same method but with different concentrations of $Fe(NO_3)_3$ (0.2, 0.5, 1.0, and 3.0 wt%) (label as PMF-800-y; y denotes percentage of $Fe(NO_3)_3$ solution). Furthermore, PMF-800-Co or PMF-800-Cl was also prepared from PMF and 1.0 wt% $Co(NO_3)_3$ or $FeCl_3$ under the same conditions, respectively.

Electrocatalytic activity evaluation. 6.0 mg of the pPMF-800 or Pt catalyst (20 wt %, Pt/C) were dissolved in a mixture (3.0 mL) of water, isopropyl alcohol, and Nafion (5.0 wt %) with a ratio of 20:1:0.075 (v/v/v) under sonication to get 2 mg/mL ink. The GCE was polished carefully with 0.3 μm alumina slurries, followed by washing in acetone, ethanol and ultrapure water successively, and then allowed to dry at room temperature. Then, a certain amount of the pPMF-800 suspension was casted onto the pretreated GCE surface with a loading amount of 1.2 mg cm^{-2}. The modified electrodes were dried under the infrared lamp before use. As a comparison, the Pt/C catalyst was prepared according to the same procedure with a loading amount of catalyst (25 μg Pt/cm^2).

For RRDE and RDE experiments, the polarization curves were obtained by performing a negative-direction sweep of potential at a rate of 5 mV s^{-1} from 1.056 V to 0.056 V (*vs* RHE) in 0.10 M $HClO_4$ or from 1.164 to 0.164 V (*vs* RHE) in 0.10 M KOH. The ring potential was set at 1.256 V in 0.10 M $HClO_4$ or 1.264 V in 0.10 M KOH, respectively.

Results and discussion

The morphology and structure of resulting pPMF-800 were characterized by transmission electron microscopy (TEM), X-ray diffraction (XRD), and Raman spectroscopy. **Fig. 1a, b and S1** show the typical TEM images of PMF and pPMF-800 at different magnifications. Compared with that of the PMF (**Figures 1a** and **S1a**), many macropores and mesopores are formed on the surface of the pPMF-800, and also more Fe_3C NPs are located into the channel of pPMF-800 (**Figures 1b** and **S1b**). Herein, we found the annealing temperature at 800 °C is the key to introduce the hierarchical pores into PMF. Lower annealing temperature (600 and 700 °C) can only produce PMFs without the obvious pores (**Figure S2**). Besides the annealing temperature, the concentration of impregnated $Fe(NO_3)_3$ solution is also an important factor in fabricating pPMF-800. We found that by increasing the concentration of $Fe(NO_3)_3$ from 0.2 to 3.0 wt%, more Fe_3C NPs can be introduced into bCNTs, and more hierarchical pores appear on the surface of the bCNTs. However, too high concentration of $Fe(NO_3)_3$ (*e.g.* 3.0 wt%) can partly destroy the microstructure of bCNTs (**Figure S3**). Consequently, 1.0 wt% $Fe(NO_3)_3$ solution is the optimal condition in both putting more NPs and introducing more hierarchical pores onto bCNTs.

The hierarchical pores produced onto the surface of bCNTs herein are probably caused by releasing the oxidative gases such as NO_2, O_2, and NO during heating $Fe(NO_3)_3$ at high temperature.[22, 23] To prove our hypothesis, the composite was also obtained by impregnating the PMF with 1.0 wt% $FeCl_3$ solution under the same conditions as that of pPMF-800 (**Figure S4**), and many pores can still be observed on surface of PMF-800-Cl. This has also been confirmed in recent reports that heating $FeCl_3{\cdot}xH_2O$ at high temperature could release H_2O, Cl_2, and HCl, promoting the formation of the pores on the carbon composites.[22, 24, 25] Moreover, to further verify more NPs were formed into the pPMF-800, PMF-800-Co was made from the pyrolysis of the PMF with 1.0 wt% $Co(NO_3)_3$ solution. **Figure 1c** shows the TEM image of the PMF-800-Co, obviously containing the hierarchical pores and more NPs. The elemental distribution of a typical PMF-800-Co was investigated using high angle annular dark field scanning transmission electron microscopy (HAADF-STEM), as shown in **Figure 1d-h**. Along the bCNTs, it is obvious that Fe (green) and Co (blue) mainly concentrate inside the bCNT, while C (red) and N (brown) distribute on the whole bCNT surface, verifying the formation of the Co-containing NPs. Hence, our impregnating procedure will not only produce more hierarchical pores along the bCNTs, but also increase the amount of transition metal-based NPs, both of which play the key roles in enhancing ORR process especially in the acidic solution.[26]

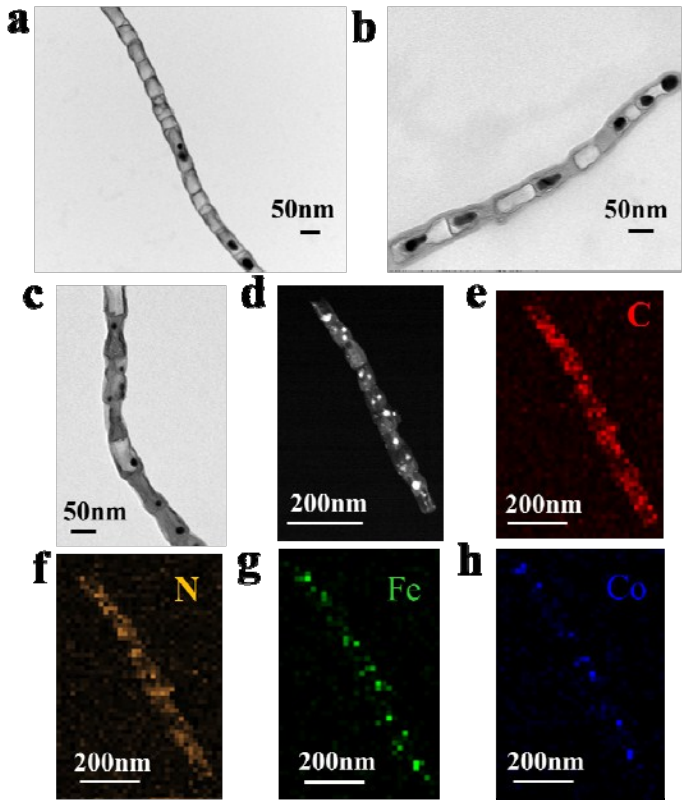

Figure 1. TEM images of the resultant (a) PMF, (b) pPMF-800, (c) PMF-800-Co, (d) HAADF-STEM, and (e-h) mapping images of the resultant PMF-800-Co.

The crystal structure of pPMF-800 was characterized by X-ray diffraction (XRD). **Figures 2a** and **S5** show the XRD patterns of the pPMF-800, PMF, N-doped multiwalled CNT (NCNT), and NCNT-800-Fe. A typical strong peak at about 26° is observed in PMF, NCNT, and NCNT-800-Fe corresponding to the (002) facets of graphite carbon, being in agreement with the structural feature of CNTs. But the peak (26°) is very weak in pPMF-800 due to the lack of ordered carbon in CNTs with hierarchical pores. The peaks located at 37.8, 43.9, 45.0, 46.0, 49.2, and 54.5° correspond to the Fe_3C (JCPDS file, No. 892867).[21] To calculate the content of Fe, the thermogravimetric analysis (TGA) of the pPMF-800 and PMF was conducted at O_2 atmosphere (**Figure 2b**). Compared with that (38.1 wt%) in PMF, the amount of Fe_3C NPs in pPMF-800 is 41.4 wt%. The porous properties of pPMF-800 and PMF were studied by the nitrogen adsorption/desorption isotherm (**Figure 2c**). Obviously, the pPMF-800 presents a bigger BET surface area (190 m^2/g) than that of PMF (151.2 m^2/g). In particular, pPMF-800 exhibits the interesting hierarchical pores with the pores size ranges 2 to 100 nm containing micro-, meso-, and macropores (the *inset* of **Figure 2c**). A Raman spectrum was used to study the graphitization degree of the resulting pPMF-800 and PMF because the D band (*ca.* 1360 cm^{-1}) and G band (*ca.* 15[illegible] cm^{-1}) can provide information on the disorder and crystallinity of sp^2 carbon materials, respectively. As shown in **Figures 2d**, **S6** and **Table S1**, pPMF-800 shows the higher I_D/I_G value of 1.01 than PMF (0.81), indicating a high degree of disordered carbon, which can be attributed to the formation of hierarchical pores along the bamboo-like microstructure. X-ray photoelectron spectroscopy (XPS) analysis (**Figure S7**) reveals that pPMF-800 is mainly composed of C, N, O, and Fe. In addition, the Fe content of pPMF-800 surface is 0.90 at.%, which is much higher than that of PMF (0.46 at.%), proving the further addition of Fe into the bCNTs.

Figure 2. (a) XRD survey, (b) TGA, (c) N_2 adsorption/desorption isotherm, and (d) Raman spectra of the resultant pPMF-800 and PMF.

The electrocatalytic activity and stability of the pPMF-800 and PMF were studied by rotating disk electrode (RDE) and rotating ring-disk electrode (RRDE) techniques. To perform these tests, the as-produced catalysts were dispersed in deionized water + isopropanol + 5% Nafion (*v:v:v* = 20:1:0.075) to reach a 2 mg/mL ink. Then, 42 μL of the catalyst ink was coated on the surface of a glassy carbon electrode and dried under an infrared lamp. The effect of $Fe(NO_3)_3$ concentrations on ORR activity of the resulting hybrid materials was investigated (**Figure 3)**, showing 1.[illegible] wt% $Fe(NO_3)_3$ solution is the optimal concentration to produce the pPMF-800 with highest ORR half-wave potential under the identical conditions in both acidic (**Figure 3a**) and alkaline (**Figure 3b**) solutions. Under the optimal conditions our pPMF-800 catalyst owns an excellent ORR activity and

durability in acidic solution. It exhibits a much better $E_{1/2}$ (0.710 V *vs* RHE) for ORR than that of PMF (0.575 V) in O_2-saturated 0.10 M $HClO_4$ solution (**Figure 4a**). Most importantly, the onset potential (E_{onset}) (0.890 V) and $E_{1/2}$ of the pPMF-800 for ORR in 0.10 M $HClO_4$ are comparable to those of the Pt/C catalyst (0.974 and 0.782 V, correspondingly, **Figure 4b**), and particularly comparable to those of previously best results (**Table S2**). The H_2O_2 yields on the pPMF-800 catalyst in acidic solution, tested by RRDE technique, are below 1.9% and the electron-transfer number (*n*) are *ca.* 3.96 over the potential range from 0.656 to 0.296 V (**Figure 4c, d**), revealing a typical 4e pathway dominated ORR process. Kinetic currents of the pPMF-800 (**Figure 4e**) derived from **Figure 4b** show a Tafel slope of 36 mV/decade at low overpotentials, close to 34 mV/decade for the Pt/C catalyst.[6] The pPMF-800 catalyst shows much better stability for ORR than the Pt/C catalyst, as revealed by a much lower ORR polarization curve change (11 mV negative shift) on the pPMF-800 (**Figure 4f**) than on the Pt/C catalyst (62 mV negative shift) (**Figure S8a**) after 3000 cycles between 1.056 and 0.056 V.

Figure 4. (a) Representative ORR polarization curves fo PMF, Pt/C and pPMF-800, (b) RRDE curves, (c) H_2O_2 yields, (d) electron transfer number (n) of pPMF-800 and Pt/C, (Tafel plots of pPMF-800 and Pt/C, and (f) ORR polarizatio curves of pPMF-800 for ORR before and after 3000 cycles. The electrolyte is O_2-saturated 0.10 M $HClO_4$, the scan an rotation rates are 5 mV/s and 1600 rpm, respectively.

Figure 3. The effect of $Fe(NO_3)_3$ concentrations on the ORR polarization curves of the PMF-800-0.2, PMF-800-0.5, PMF-800-1, PMF-800-3, and PMF in O_2-saturated (a) 0.10 M $HClO_4$ and (b) 0.10 M KOH aqueous solutions with a scan rate of 5 mV/s and a rotation rate of 1600 rpm.

More interestingly, our new pPMF-800 catalyst is also extremely active for ORR in alkaline solution. **Figure a** shows representative ORR polarization curves for PMF, Pt/C, and pPMF-800 in O_2-saturated 0.10 M KOH solution. It is found that relative to those of PMF and Pt/C, the pPMF-80 exhibits more positive E_{onset} and $E_{1/2}$ in 0.10 M KOH indicating that introduction of more active Fe_3C NPs and hierarchical pores are very important for further enhancin the ORR performance of PMF. **Figure 5b** displays typica RRDE voltammograms of pPMF-800 and commercial Pt/C catalyst in O_2-saturated 0.10 M KOH solution. We can se that the pPMF-800 catalyst shows much higher electrocatalytic activity for ORR than the commercial Pt/C, a indicated by its $E_{1/2}$ 67 mV more positive than that of the Pt/C RRDE test results (**Figure 5c**) also exhibit that the H_2O yields measured with the pPMF-800 catalyst remain belo 1.5% at all potentials in 0.10 M KOH, corresponding to high *n* of 3.99 (**Figure 5d**), confirming its high ORR catal efficiency. **Figure 5e** displays the Tafel plots of pPMF-8

and commercial Pt/C. The pPMF-800 catalyst has a Tafel slope of 32 mV/decade in 0.10 M KOH, close to the 30 mV/decade of the Pt/C, illustrating that it has an excellent kinetic process for ORR. Furthermore, as demonstrated in **Figures 5f and S8b**, the pPMF-800 catalyst also exhibits high durability in alkaline solution for ORR, confirmed by its small ORR polarization curve shift (6 mV) after 3000 cycles between 0.164 to 1.164 V, while there was a 23 mV loss of $E_{1/2}$ for the Pt/C catalyst under the same conditions, proving the superior stability of the pPMF-800 catalyst.

Figure 5. (a) Representative ORR polarization curves for PMF, Pt/C and pPMF-800, (b) RRDE curves, (c) H_2O_2 yield, (d) electron transfer number (n) of pPMF-800 and Pt/C, (e) Tafel plots of pPMF-800 and Pt/C, and (f) ORR polarization curves of pPMF-800 for ORR before and after 3000 cycles. The electrolyte is O_2-saturated 0.10 M KOH, the scan and rotation rates are 5 mV/s and 1600 rpm, respectively.

Except for the high percentage of N (5.64 at.% from XPS spectra in **Figure S7**) doped in the pPMF-800, we think that three more important aspects should be responsible for the superior ORR performances of pPMF-800 in both acidic and alkaline solutions: (1) 3D hierarchical porous textures with micro-, meso-, and macropores can not only further enhance the accessible specific surface area of the materials, but also facilitate fast diffusion of electrolyte and O_2 to active sites.[8, 27, 28] (2) A large amount of hierarchical pores along the bCNTs can offer more graphene-like edges, thus introducing massive active sites for ORR process.[29-31] (3) The increased amount of electrochemically active Fe_3C NPs into the channel of bCNTs can further enhance ORR activity which make the outer surface of the carbon layer more active to ORR.[21, 32-35]

To testify the universal of this impregnating method to the CNT structure, we produced the NCNT-800-Fe from traditional NCNT under the same conditions, the ORR activity of NCNT-800-Fe increases significantly in both acidic and basic solutions compared with un-treated NCNT (**Figure S9)**. Hence, it is a general way to enhance the ORR activity by the introduction of more electrochemically active and stable Fe_3C NPs into CNTs.

In summary, we design a new one-step synthetic strategy for the controlled synthesis of hierarchical porous bCNT/Fe_3C NPs hybrid nanoelectrocatalysts for enhancing ORR performance by impregnating the PMF with $Fe(NO_3)_3$ solution, and followed by the calcination of composite in N_2 atmosphere at 800 ^oC. The key part of our synthesis is that during the impregnating process, $Fe(NO_3)_3$ can be driven into the channels of bCNTs by capillary forces, and then at high temperature, the oxidative etching of the produced gases such as NO_2, O_2, and NO by heating $Fe(NO_3)_3$ makes bCNTs have the interesting hierarchical micro-, meso-, and macropores. The pPMF-800 exhibits much higher activity and stability for ORR than the un-treated PMF catalyst, especially in acidic solution, making it one of the best non-precious-metal catalysts. This work paves the way to the development of an economical and efficient protocol to construct novel active and stable hierarchical porous carbon/Fe_3C NPs hybrids for applications in fuel cells, lithium-ion batteries, sensors, supercapacitors, and beyond.

Acknowledgement

This work was financially supported by the Ministry of Science and Technology of China (No. 2013YQ170585), the start-up funding from Peking University and Young Thousand Talented Program.

References

1.Y. Zhao, K. Kamiya, K. Hashimoto, S. Nakanishi, *J. Phys. Chem. C* 2015, *119*, 2583.
2.K. P. Singh, E. J. Bae, J. S. Yu, *J. Am. Chem. Soc.* 2015, *137*, 3165.
3.W. Niu, L. Li, X. Liu, N. Wang, J. Liu, W. Zhou, Z. Tang, S. Chen, *J. Am. Chem. Soc.* 2015, *137*, 5555.

4.H. X. Zhong, J. Wang, Y. W. Zhang, W. L. Xu, W. Xing, D. Xu, Y. F. Zhang, X. B. Zhang, *Angew. Chem. Int. Ed.* 2014, *53*, 14235.
5.K. Gong, F. Du, Z. Xia, M. Durstock, L. Dai, *Science* 2009, *323*, 760.
6.Y. Liang, Y. Li, H. Wang, J. Zhou, J. Wang, T. Regier, H. Dai, *Nat. Mater.* 2011, *10*, 780.
7.C. H. Choi, M. W. Chung, H. C. Kwon, S. H. Park, S. I. Woo, *J. Mater. Chem. A* 2013, *1*, 3694.
8.Z. Liu, H. Nie, Z. Yang, J. Zhang, Z. Jin, Y. Lu, Z. Xiao, S. Huang, *Nanoscale* 2013, *5*, 3283.
9.Z. Ma, S. Dou, A. Shen, L. Tao, L. Dai, S. Wang, *Angew. Chem. Int. Ed.* 2015, *54*, 1888.
10.M. Lefevre, E. Proietti, F. Jaouen, J. P. Dodelet, *Science* 2009, *324*, 71.
11.S. Maldonado, K. J. Stevenson, *J. Phys. Chem. B* 2005, *109*, 4707.
12.Y. Y. Wei, S. Q. Chen, D. W. Su, B. Sun, J. G. Zhu, G. X. Wang, *J. Mater. Chem. A* 2014, *2*, 8103.
13.S. Han, D. Wu, S. Li, F. Zhang, X. Feng, *Adv. Mater.* 2014, *26*, 849.
14.Y. J. Si, C. G. Chen, W. Yin, H. Cai, *Chinese Chem. Lett.* 2010, *21*, 983.
15.D. Liu, X. Zhang, Z. Sun, T. You, *Nanoscale* 2013, *5*, 9528.
16.W. Ding, Z. Wei, S. Chen, X. Qi, T. Yang, J. Hu, D. Wang, L.-J. Wan, S. F. Alvi, L. Li, *Angew. Chem. Int. Ed.* 2013, *52*, 11755.
17.L. Dai, Y. Xue, L. Qu, H. J. Choi, J. B. Baek, *Chem. Rev.* 2015, *115*, 4823.
18.Y. Wang, A. Kong, X. Chen, Q. Lin, P. Feng, *ACS Catal.* 2015, *5*, 3887.
19.Z. Y. Wu, X. X. Xu, B. C. Hu, H. W. Liang, Y. Lin, L. F. Chen, S. H. Yu, *Angew. Chem. Int. Ed.* 2015, 54, 8179.
20.Y. J. Sa, C. Park, H. Y. Jeong, S.-H. Park, Z. Lee, K. T. Kim, G.-G. Park, S. H. Joo, *Angew. Chem. Int. Ed.* 2014, *53*, 4102.
21.W. Yang, X. Liu, X. Yue, J. Jia, S. Guo, *J. Am. Chem. Soc.* 2015, *137*, 1436.
22.M. Sobiesiak, *Adsorption* 2013, *19*, 349.
23.W. Yang, Y. Zhang, C. Liu, J. Jia, *J. Power Sources* 2015, *274*, 595.
24.S. B. Kanungo, S. K. Mishra, *J. Therm. Anal. Calorim.* 1996, *46*, 1487.
25.E. S. Freeman, *J. Am. Chem. Soc.* 1957, *79*, 838.
26.W. Yang, X. Yue, X. Liu, J. Zhai, J. Jia, *Nanoscale* 2015, *7*, 11956.
27.J. Wang, R. Ma, Z. Zhou, G. Liu, Q. Liu, *Sci. Rep.* 2015, *5*, 9304.
28.Y. Li, H. Zhang, Y. Wang, P. Liu, H. Yang, X. Yao, D. Wang, Z. Tang, H. Zhao, *Energ. Environ. Sci.* 2014, *7*, 3720.
29.H.-W. Liang, W. Wei, Z.-S. Wu, X. Feng, K. Muellen, *J. Am. Chem. Soc.* 2013, *135*, 16002.
30.Z. Lin, G. H. Waller, Y. Liu, M. Liu, C.-P. Wong, *Nano Energy* 2013, *2*, 241.
31.J. Liang, Y. Jiao, M. Jaroniec, S. Z. Qiao, *Angew. Chem. Int. Ed.* 2012, *51*, 11496.
32.Y. Hu, J. O. Jensen, W. Zhang, L. N. Cleemann, W. Xing, N. J. Bjerrum, Q. Li, *Angew. Chem. Int. Ed.* 2014, *53*, 3675.
33.W. Yang, Y. Zhai, X. Yue, Y. Wang, J. Jia, *Chem. Commun.* 2014, *50*, 11151.
34.J. Wang, G. Wang, S. Miao, X. Jiang, J. Li, X. Bao, *Carbon* 2014, *75*, 381.
35.R. Zhang, S. He, Y. Lu, W. Chen, *J. Mater. Chem. A* 2015, *3*, 3559.